Enabling Low-Complexity MIMO in FBMC-OQAM

Ronald Nissel[†,‡] and Markus Rupp[†]
[†] Institute of Telecommunications, Technische Universität Wien, Vienna, Austria
[‡] Christian Doppler Laboratory for Dependable Wireless Connectivity for the Society in Motion, ITC, TU Wien
Email: {rnissel, mrupp}@nt.tuwien.ac.at

***Abstract*—Filter Bank Multi-Carrier (FBMC) offers superior spectral properties compared to Orthogonal Frequency Division Multiplexing (OFDM), at the cost of imaginary interference, which makes the application of Multiple-Input and Multiple-Output (MIMO) more challenging. By spreading symbols in time (or frequency), we can completely eliminate the imaginary interference, so that all MIMO techniques known in OFDM can be straightforwardly applied in FBMC. The spreading process itself has low complexity because it is based on Hadamard matrices. Although spreading allows to restore complex orthogonality in FBMC within one transmission block, we observe interference from neighboring blocks. By including a guard time-slot, the signal-to-interference ratio can be further improved. Furthermore, we investigate the effect of a time-variant channel on such spreading approach. Finally, testbed measurements show the applicability of our FBMC based MIMO transmission scheme in real world environments.**

I. Introduction

The next generation of wireless systems (5G) should support a large range of possible use cases, for example, low latency communication or machine type communication [1]. This requires a more flexible assignment of the available time-frequency resources, not possible in conventional Orthogonal Frequency Division Multiplexing (OFDM) due to its bad spectral behavior. We thus need new waveforms (or derivatives of OFDM), such as windowed OFDM or Universal Filtered Multi-Carrier (UFMC) [2]. Another method with even better spectral properties is Filter Bank Multi-Carrier (FBMC) with Offset Quadrature Amplitude Modulation (OQAM), in short just FBMC, which usually employs pulses that are localized in both, time and frequency, at the expense of replacing the complex orthogonality condition with the less strict real orthogonality condition [3]. Although FBMC behaves in many aspects similar to OFDM, some techniques become more challenging due to the imaginary interference, for example, channel estimation [4] or Multiple-Input and Multiple-Output (MIMO) [5]. There exist many works which combine MIMO and FBMC but most of them have serious drawbacks, such as [6] which relies on channel information at the transmitter or [7] which requires high computational complexity.

A more elegant method to combine MIMO with FBMC is to spread symbols in the time (or frequency) domain, which allows us to cancel the imaginary interference. Authors in [5] use a Fast Fourier Transform (FFT) spreading which, however, has the disadvantage of residual interference and increased complexity due to the additional FFT. A better solution is to spread symbols with a reduced Hadamard matrix because it requires no multiplications so that the additional complexity becomes very low. Such approach was first suggested in [8] and later applied by the same authors in [9] to combine FBMC with Alamouti's space-time block coding. After the spreading and despreading process, we can straightforwardly apply all MIMO methods known in OFDM, resulting in the same MIMO complexity.

Our paper is based on the idea of [8], [9] with the following novel contributions:

- We reformulate the Hadamard spreading approach in matrix notation, allowing additional analytical insights.
- While [8], [9] considered only the transmission of one block, we investigate the interference between different blocks and propose the usage of guard symbols.
- In contrast to [8], [9], we allow for a time-variant channel and derive closed-form Signal-to-Interference Ratio (SIR) expressions.
- The MATLAB code used in this paper can be downloaded at https://www.nt.tuwien.ac.at/downloads/ and supports reproducibility of our results.
- We validate our MIMO approach in real world measurements by employing the Vienna Wireless Testbed [10], [11].

II. FBMC-OQAM

In multicarrier transmissions, symbols $x_{l,k}$ are transmitted over a rectangular time-frequency grid, with l denoting the subcarrier-position and k the time-position. The transmitted signal $s(t)$ of a transmission block consisting of L subcarriers and K multicarrier symbols can be written as

$$s(t) = \sum_{k=1}^{K} \sum_{l=1}^{L} g_{l,k}(t)\, x_{l,k}, \tag{1}$$

where $g_{l,k}(t)$ denotes the basis pulse, essentially, a time and frequency shifted version of the prototype filter $p(t)$:

$$g_{l,k}(t) = p(t - kT)\, \mathrm{e}^{\mathrm{j}2\pi\, lF\,(t-kT)}\, \mathrm{e}^{\mathrm{j}\theta_{l,k}}, \tag{2}$$

with T being the time spacing and F the frequency spacing (subcarrier spacing). The received symbols $y_{l,k}$ are then obtained by projecting the received signal $r(t)$ onto the basis pulses $g_{l,k}(t)$

$$y_{l,k} = \langle r(t), g_{l,k}(t) \rangle = \int_{-\infty}^{\infty} r(t) g_{l,k}^{*}(t)\, \mathrm{d}t. \tag{3}$$

A desired property of the basis pulses $g_{l,k}$ is orthogonality, that is, $\langle g_{l_1,k_1}(t), g_{l_2,k_2}(t) \rangle = \delta_{(l_1-l_2),(k_1-k_2)}$, because it simplifies the detection process. Unfortunately, it is not possible to find

basis pulses $g_{l,k}(t)$ which are (complex) orthogonal, have maximum spectral efficiency of $TF = 1$, and are localized in both, time and frequency, according to the Balian-Low theorem [12]. In OFDM, $\theta_{l,k} = 0$, the prototype filter is usually based on a rectangular function. Thus, frequency localization is not fulfilled. Additionally, a Cyclic Prefix (CP) is often added in practice, so that the orthogonality condition transforms to a bi-orthogonality condition (transmit and receive pulses are different) and spectral efficiency is sacrificed, $TF > 1$, in order to gain robustness in frequency selective channels.

In FBMC, we satisfy the Balian-Low theorem by replacing the complex orthogonality condition with the less strict real orthogonality condition, so that only real-valued symbols, $x_{l,k} \in \mathbb{R}$, can be transmitted. The idea is to design a prototype filter which is (complex) orthogonal for a time-frequency spacing of $TF = 2$. See for example [13] for such a pulse, based on Hermite polynomials. The time spacing as well as the frequency spacing is then reduced by a factor of two, $TF = \frac{1}{2}$ (real symbols), which is equivalent to $TF = 1$ (complex symbols) in terms of transmitted information per time unit. Such time-frequency squeezing causes interference which, however, is shifted to the purely imaginary domain by the phase shift $\theta_{l,k} = \frac{\pi}{2}(l+k)$. By taking the real part we can then completely eliminate this imaginary interference.

In order to simplify analytical investigations, we reformulate our transmission system model in matrix notation. Sampling the transmitted signal $s(t)$ and writing it in a vector allows us to reformulate (1) by

$$\mathbf{s} = \mathbf{G}\mathbf{x}, \tag{4}$$

where the column vectors of $\mathbf{G}$ represent the sampled basis pulses $g_{l,k}(t)$, written in matrix notation so that it corresponds to the transmitted symbol vector $\mathbf{x} \in \mathbb{C}^{LK\times 1}$, defined as:

$$\mathbf{x} = \mathrm{vec}\left\{\begin{bmatrix} x_{1,1} & \cdots & x_{1,K} \\ \vdots & \ddots & \vdots \\ x_{L,1} & \cdots & x_{L,K} \end{bmatrix}\right\} \tag{5}$$

$$= \begin{bmatrix} x_{1,1} & x_{2,1} & \cdots & x_{L,1} & x_{1,2} & \cdots & x_{L,K} \end{bmatrix}^{\mathsf{T}}. \tag{6}$$

In practice, (4) is calculated by an FFT together with a polyphase network and not by a matrix multiplication [14]. However, expressing the system in such a way provides additional analytical insights. Stacking the received symbols $y_{l,k}$ in a vector $\mathbf{y} \in \mathbb{C}^{LK\times 1}$,

$$\mathbf{y} = \begin{bmatrix} y_{1,1} & y_{2,1} & \cdots & y_{L,1} & y_{1,2} & \cdots & y_{L,K} \end{bmatrix}^{\mathsf{T}}, \tag{7}$$

and assuming an Additive White Gaussian Noise (AWGN) channel (in Section V we will consider a more general case), allows us to reformulate our transmission system model of (3) in matrix notation as

$$\mathbf{y} = \mathbf{G}^{\mathsf{H}}\mathbf{r} = \mathbf{D}\mathbf{x} + \mathbf{n}, \tag{8}$$

with $\mathbf{n} \sim \mathcal{CN}(\mathbf{0}, P_{\mathrm{n}}\,\mathbf{D})$ being the random noise and $\mathbf{D}$ the transmission matrix, defined as

$$\mathbf{D} = \mathbf{G}^{\mathsf{H}}\mathbf{G}. \tag{9}$$

In OFDM, the transmission matrix is an identity matrix, that is, $\mathbf{D} = \mathbf{I}_{LK}$. In FBMC, on the other hand, we observe imaginary interference at the off-diagonal elements and only by taking the real part, we end up with an identity matrix, that is, $\Re\{\mathbf{D}\} = \mathbf{I}_{LK}$. An example for such FBMC transmission matrix can be found in the appendix. By investigating (8), a natural question is whether we lose any information in FBMC by taking the real part. The answer is no! This can easily be shown by an eigenvalue decomposition of the transmission matrix $\mathbf{D} = \mathbf{G}^{\mathsf{H}}\mathbf{G} = \mathbf{U}\mathbf{\Lambda}\mathbf{U}^{\mathsf{H}}$, with the unitary matrix $\mathbf{U}$. For $L \to \infty$ and $K \to \infty$ (thus ignoring any edge effects), $\mathbf{D}$ has exactly $\frac{LK}{2}$ nonzero eigenvalues, each having a value of 2. Therefore we can transmit only $\frac{LK}{2}$ complex symbols, which is equivalent to the transmission of LK real symbols. Additionally, we observe the same Signal-to-Noise Ratio (SNR). Thus, from an information theoretic point of view, OFDM (without CP), FBMC and precoded FBMC (with $\mathbf{U}$) exhibit the same rate. If $L < \infty$ or $K < \infty$, the rate may differ, depending on the required guard resources in time and frequency.

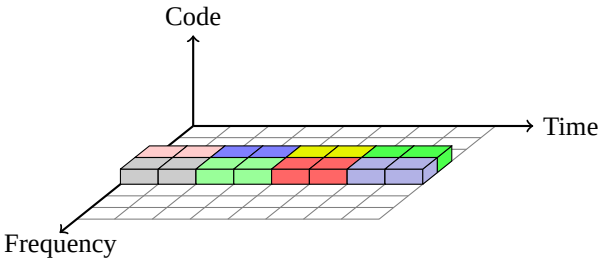

Fig. 1. In FBMC-OQAM each time-frequency position can only carrier real symbols, so that we need two time slots to transmit one complex symbol (thus the name offset QAM).

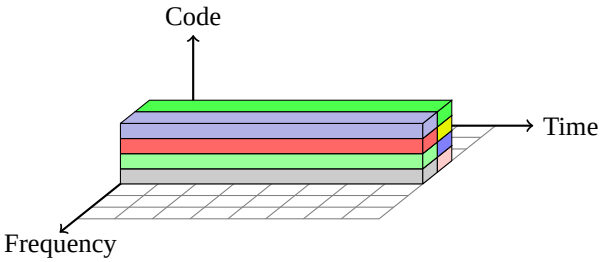

Fig. 2. In coded FBMC-OQAM we spread a complex symbol over several time slots which allows us to cancel the imaginary interference, restoring complex orthogonality. Because the spreading is based on Hadamard matrices, the additional complexity becomes very low. Note that we can equivalently spread over the frequency domain.

III. Coded FBMC-OQAM

Figure 1 shows the concept of conventional FBMC transmissions. Real-valued symbols are transmitted over a rectangular time-frequency grid. The main problem of such FBMC transmission scheme is the imaginary interference, see Section II. Although in many cases, especially in Single-Input and Single-Output (SISO) systems, we can easily get rid of this imaginary interference, simply by taking the real part; in many MIMO applications this is not possible. We can avoid this problem by spreading data symbols over several time positions, see Figure 2, which allows us to eliminate

the imaginary interference and to transmit complex-valued symbols. The uncorrelated data symbols $\tilde{\mathbf{x}}$ are precoded by a unitary coding/spreading matrix $\mathbf{C}$, so that the transmitted symbols $\mathbf{x}$ are calculated as

$$\mathbf{x} = \mathbf{C}\,\tilde{\mathbf{x}}. \tag{10}$$

The received data symbols $\tilde{\mathbf{y}}$, on the other hand, are obtained by decoding of the received symbols according to

$$\tilde{\mathbf{y}} = \mathbf{C}^{\mathsf{H}}\,\mathbf{y}. \tag{11}$$

In order to cancel the imaginary interference, the coding matrix has to be chosen so that the following condition is fulfilled,

$$\mathbf{C}^{\mathsf{H}}\,\mathbf{D}\,\mathbf{C} = \mathbf{I}, \tag{12}$$

As already mentioned in Section II, it is possible to satisfy (12) by applying an eigenvalue decomposition $\mathbf{D} = \mathbf{U}\mathbf{\Lambda}\mathbf{U}^{\mathsf{H}}$ and choosing the first $\frac{LK}{2}$ column vectors of $\mathbf{U}$ as our coding matrix $\mathbf{C} \in \mathbb{C}^{LK\times\frac{LK}{2}}$. The problem with such approach is the high computational complexity and that the spreading is performed in both, time and frequency, which only works for a doubly-flat channel. A better method was found in [8] and is based on Hadamard matrices. Here, we take $\frac{K}{2}$ suitable column vectors out of a $K \times K$ Hadamard matrix and spread with them our symbols in the time domain, see Figure 2. We do this for all subcarriers, so that we find a coding matrix $\mathbf{C} \in \mathbb{R}^{LK\times\frac{LK}{2}}$ which satisfies (12). In the appendix we present a simple example of such matrix. Authors of [8] left the question open whether it is possible to find a coding matrix that has more than $\frac{LK}{2}$ columns while still satisfying (12). The eigenvalue decomposition of $\mathbf{D}$ shows that this is not possible (ignoring edge effects which become negligible for a large number of K and L). A small disadvantage of Hadamard spreading is the fact that the coding length has to be a power of two. This makes the integration into existing systems problematic but has almost no impact if a system is designed from scratch. The big advantage of Hadamard spreading, on the other hand, is that only additions but no multiplications are required, so that the additional complexity becomes very low. Indeed, for each data symbol, we only need $\log_2(K)-1$ extra additions/subtractions at the transmitter and $\log_2(K)$ extra additions/subtractions at the receiver. However, we should keep in mind that the overall complexity of FBMC is approximately two to five times higher than in OFDM. Note that Hadamard spreading has almost no influence on the power spectral density, besides a few small ripples, see Figure 3, so that the superior spectral properties of FBMC are preserved. If a low latency transmission is required, the spreading can equivalently be performed in the frequency domain, or the subcarrier spacing can be increased.

According to the Balian-Low theorem, it is not possible to satisfy several desired properties (see Section II) simultaneously, so that at least one has to be sacrificed. For example, the FBMC-QAM method in [15] leads to an even worse spectral behavior than in OFDM, as shown by authors in [16], who also propose an FBMC-QAM transmission scheme

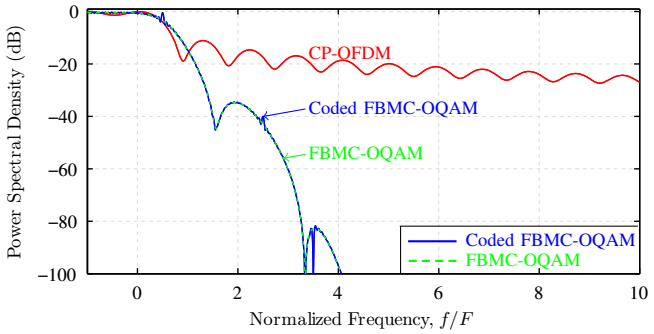

Fig. 3. The superior spectral properties of FBMC are preserved even if we apply Hadamard spreading. Note that the transmit power has a similar shape as the power spectral density due to the Hermite prototype filter [13].

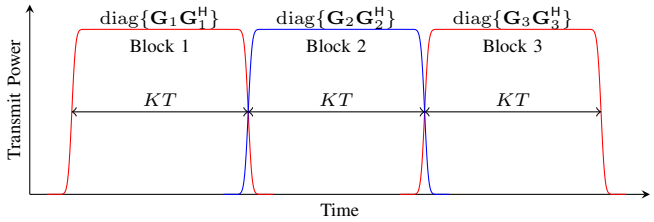

Fig. 4. Neighboring blocks cause interference. In conventional FBMC-OQAM, such interference can be completely eliminated by taking the real part. In coded FBMC-OQAM, however, this interference remains, see Figure 5, and affects the performance if the interference power is higher than the noise power. In a logarithmic scale, the shape would be similar as in Figure 3.

but they ignore time-localization and sacrifice orthogonality (SIR $\approx$ 20 dB). Coded FBMC-OQAM, on the other hand, has maximum spectral efficiency, time-localization, frequency-localization and orthogonality! Unfortunately, this also comes at a price, namely, the spreading of symbols in time, which, however, is perfectly feasible in practice because symbols are already clustered together to keep the signaling overhead low. Nonetheless, there are some important implications which need to be considered, see Section IV and V.

IV. Block-interference

So far, we assumed a block transmission consisting of L subcarriers and K FBMC symbols. In theory, K can approach infinity. However, because we spread symbols over K time slots, this is not practical due to latency constraints and the fact that the channel varies over time, destroying orthogonality, see Section V. We therefore have to consider block-wise transmissions. For analytical investigations, it is sufficient to assume three transmit blocks and to analyze the performance in block 2. The first block is characterized by the transmit matrix $\mathbf{G}_1$, the second block by $\mathbf{G}_2$ and the third block by $\mathbf{G}_3$, whereas these transmit matrices are almost the same except that they are time shifted by KT from each other, see Figure 4. The overall transmit signal can then be written as

$$\mathbf{s} = \begin{bmatrix}\mathbf{G}_1 & \mathbf{G}_2 & \mathbf{G}_3\end{bmatrix}\begin{bmatrix}\mathbf{x}_1\\ \mathbf{x}_2\\ \mathbf{x}_3\end{bmatrix}, \tag{13}$$

where $\mathbf{x}_1 \in \mathbb{C}^{LK\times 1}$ represents the transmitted symbols of the first block, $\mathbf{x}_2$ of the second block and $\mathbf{x}_3$ of the third

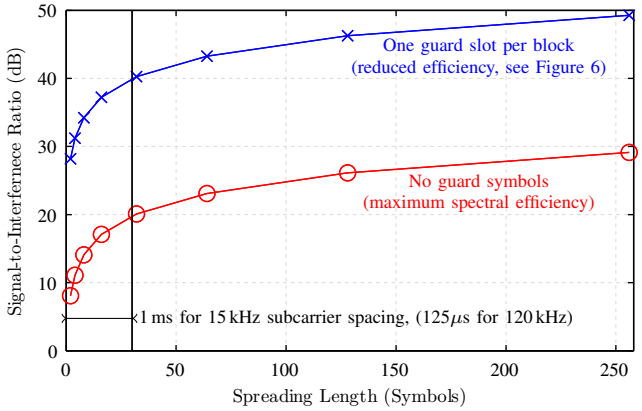

Fig. 5. We observe interference from neighboring blocks due to the small overlapping between blocks, see Figure 4. By including a guard slot, we increase the SIR by approximately 20 dB at the expense of decreased spectral efficiency, see Figure 6. Because our prototype filter is symmetric in time and frequency, the SIR values here also apply for frequency spreading. Note that the spreading length has to be a power of two due to the Hadamard structure.

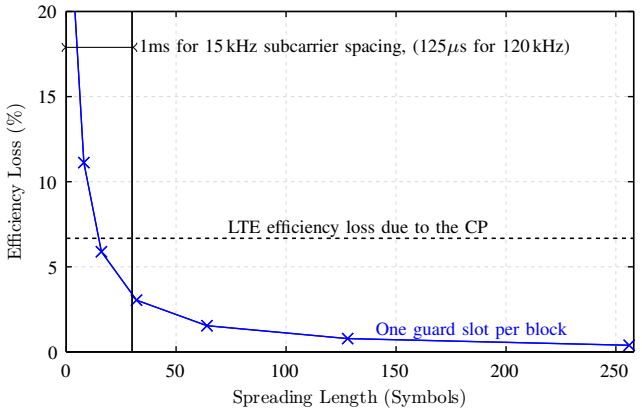

Fig. 6. Adding a guard slot reduces the spectral efficiency. However, for a high spreading length, the efficiency loss $\frac{1}{K+1}$ approaches zero.

block. As shown in Figure 4, these blocks overlap slightly. In conventional FBMC, such overlapping has no influence on the performance due to the real orthogonality condition, that is $\Re\{\mathbf{G}_2^{\mathsf{H}}\mathbf{G}_1\} = \Re\{\mathbf{G}_2^{\mathsf{H}}\mathbf{G}_3\} = \mathbf{0}_{LK}$. Unfortunately, this no longer holds true if we apply time spreading within one transmission block, as described in Section III. By ignoring the noise, we obtain the received data symbols of block 2 by:

$$\tilde{\mathbf{y}}_2 = \mathbf{C}^{\mathsf{H}}\mathbf{G}_2^{\mathsf{H}}\mathbf{s} \tag{14}$$

$$= \tilde{\mathbf{x}}_2 + \mathbf{C}^{\mathsf{H}}\mathbf{G}_2^{\mathsf{H}}\mathbf{G}_1\mathbf{C}\,\tilde{\mathbf{x}}_1 + \mathbf{C}^{\mathsf{H}}\mathbf{G}_2^{\mathsf{H}}\mathbf{G}_3\mathbf{C}\,\tilde{\mathbf{x}}_3. \tag{15}$$

The first term in (15) represents the signal power while the second and third term the undesired interference. The SIR of block 2 can thus be expressed by:

$$\mathrm{SIR}_2 = \frac{\frac{KL}{2}}{\sum_{m=1}^{\frac{KL}{2}}\sum_{n=1}^{\frac{KL}{2}} \left|[\mathbf{C}^{\mathsf{H}}\mathbf{G}_2^{\mathsf{H}}\mathbf{G}_1\mathbf{C}]_{m,n}\right|^2 + \left|[\mathbf{C}^{\mathsf{H}}\mathbf{G}_2^{\mathsf{H}}\mathbf{G}_3\mathbf{C}]_{m,n}\right|^2}, \tag{16}$$

where $[\cdot]_{m,n}$ denotes the matrix element at position (m,n) and $|\cdot|$ the absolute value. Figure 5 shows the SIR for a different number of FBMC symbols per block (spreading length). As long as the SNR is much smaller than the SIR, block interference can be neglected because the interference is dominated by the noise. Interference between blocks occurs only at the boarder region, so that, by increasing the spreading length K, we increase the SIR because the interference is spread over a higher number of symbols. However, if a short spreading length is required, the interference might be too high. By inserting a guard slot in time, we can improve the SIR, see Figure 5, at the expense of spectral efficiency, see Figure 6. The efficiency loss decreases for an increased spreading length. For comparison we also include the efficiency loss caused by the CP in OFDM (LTE). Note, however, that the overall spectral efficiency loss in OFDM is higher than illustrated in Figure 6 because OFDM needs a larger guard band than FBMC, see [13].

V. Time-Variant Channels

Wireless channels are highly underspread [17], that is, the product of the Root Mean Square (RMS) delay spread and the RMS Doppler spread is much smaller than one, so that multi-path induced interference can usually be neglected in multicarrier systems if the subcarrier spacing is chosen appropriately. Additionally, a simple one-tap equalizer is sufficient. In many cases, this is even true if we spread symbols in time, as we will see in this section.

Let us include multi-path fading in our transmission model by a time-variant convolution matrix $\mathbf{H}$. Ignoring noise, we can express the received data symbol at subcarrier position $l = 1 \ldots L$ and code position $i = 1 \ldots \frac{K}{2}$ for transmission block 2 by:

$$\tilde{y}_{l,i,2} = \underbrace{\mathbf{c}_{l,i}^{\mathsf{H}}\mathbf{G}_2^{\mathsf{H}}}_{\mathbf{a}_{l,i,2}^{\mathsf{H}}}\,\mathbf{H}\,\underbrace{\begin{bmatrix}\mathbf{G}_1\mathbf{C} & \mathbf{G}_2\mathbf{C} & \mathbf{G}_3\mathbf{C}\end{bmatrix}}_{\mathbf{B}}\begin{bmatrix}\tilde{\mathbf{x}}_1\\ \tilde{\mathbf{x}}_2\\ \tilde{\mathbf{x}}_3\end{bmatrix} \tag{17}$$

$$= \left(\begin{bmatrix}\tilde{\mathbf{x}}_1\\ \tilde{\mathbf{x}}_2\\ \tilde{\mathbf{x}}_3\end{bmatrix}^{\mathsf{T}}\mathbf{B}^{\mathsf{T}} \otimes \mathbf{a}_{l,i,2}^{\mathsf{H}}\right)\mathrm{vec}\{\mathbf{H}\}, \tag{18}$$

where $\mathbf{c}_{l,i} \in \mathbb{R}^{LK\times 1}$ denotes the $l + L(i-1)$-th column vector of $\mathbf{C}$ and corresponds to code position i and subcarrier position l. With $\otimes$ denoting the Kronecker product, we can rewrite (17) by (18) which greatly simplifies statistical investigations. Using (18) we calculate the signal plus noise power $\mathrm{P}_{\mathrm{S+I}_{l,i,2}} = \mathbb{E}\{|\tilde{y}_{l,i,2}|^2\}$ by

$$\mathrm{P}_{\mathrm{S+I}_{l,i,2}} = \mathrm{tr}\left\{\left(\mathbf{B}^{\mathsf{T}} \otimes \mathbf{a}_{l,i,2}^{\mathsf{H}}\right)\mathbf{R}_{\mathrm{vec}\{\mathbf{H}\}}\left(\mathbf{B}^{\mathsf{T}} \otimes \mathbf{a}_{l,i,2}^{\mathsf{H}}\right)^{\mathsf{H}}\right\}, \tag{19}$$

where $\mathbf{R}_{\mathrm{vec}\{\mathbf{H}\}} = \mathbb{E}\{\mathrm{vec}\{\mathbf{H}\}\mathrm{vec}\{\mathbf{H}\}^{\mathsf{H}}\}$ denotes the correlation matrix and can easily be calculated for a given power delay profile and a given power spectral density. Similar to (19), we find the signal power by

$$\mathrm{P}_{\mathrm{S}_{l,i,2}} = \left(\mathbf{a}_{l,i,2}^{\mathsf{T}} \otimes \mathbf{a}_{l,i,2}^{\mathsf{H}}\right)\mathbf{R}_{\mathrm{vec}\{\mathbf{H}\}}\left(\mathbf{a}_{l,i,2}^{\mathsf{T}} \otimes \mathbf{a}_{l,i,2}^{\mathsf{H}}\right)^{\mathsf{H}}, \tag{20}$$

so that the average SIR for the received data symbols in block

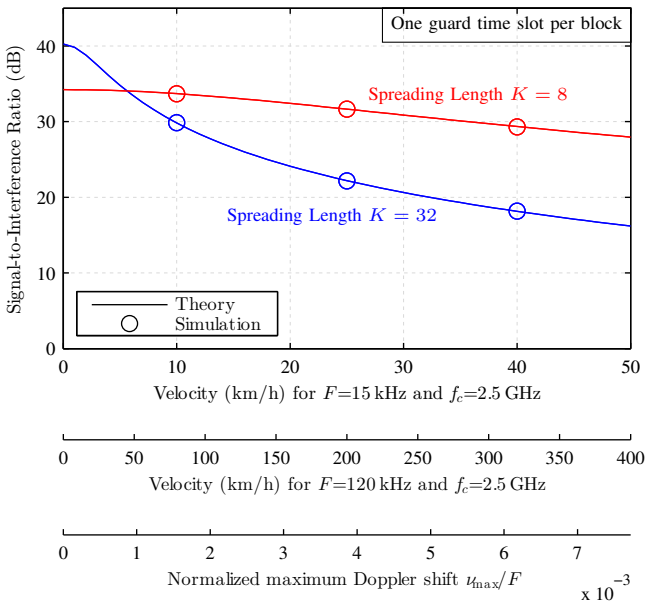

Fig. 7. A higher velocity reduces the SIR because the spreading approach assumes a time-invariant channel. By reducing the subcarrier spacing F or reducing the spreading length K, we can increase the robustness. Our theoretical SIR expression in (21) is also validated by simulations.

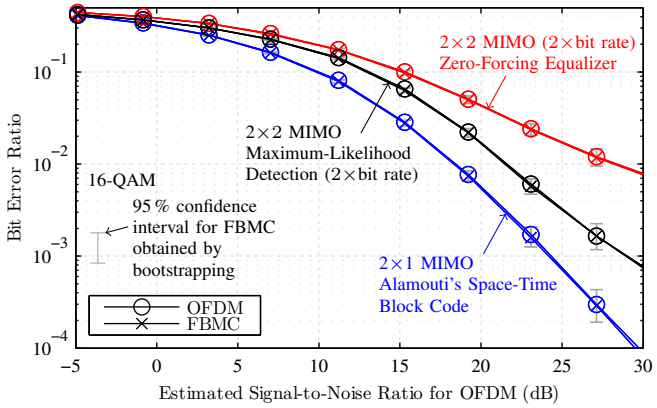

Fig. 8. Real world MIMO measurements show that FBMC-OQAM based on spreading performs exactly the same as conventional OFDM in terms of BER. Such FBMC scheme has approximately the same MIMO complexity as OFDM, but the additional advantage of better spectral properties. Perfect channel knowledge is not available in real world transmissions, so that we employ pilot symbol aided channel estimation, similar as in LTE.

2 becomes:

$$\mathrm{SIR}_2 = \frac{\sum_{l=1}^{L}\sum_{i=1}^{\frac{K}{2}} \mathrm{P}_{\mathrm{S}_{l,i,2}}}{\sum_{l=1}^{L}\sum_{i=1}^{\frac{K}{2}} \left(\mathrm{P}_{\mathrm{S+I}_{l,i,2}} - \mathrm{P}_{\mathrm{S}_{l,i,2}}\right)}. \tag{21}$$

If the channel is approximately frequency flat within one subcarrier (supported by our measurements) and for a Jakes Doppler spectrum, Figure 7 shows the SIR. The performance depends on the normalized maximum Doppler shift, defined as $f_c \frac{v}{c} \frac{1}{F}$, with f_c being the carrier frequency, v the velocity and c the speed of light. Note that we assume one guard slot per block, see Section IV, so that, for a velocity of zero, we obtain the same SIR as the blue curve in Figure 5. The smaller the spreading length, the less effect has a time-variant channel. Therefore both curves in Figure 7 intersect at some point.

VI. Real World MIMO Measurements

The main reason for spreading symbols over several time slots, as discussed in Section III, is to enable MIMO transmissions in FBMC with approximately the same MIMO complexity as in OFDM. In this section, we validate our approach by employing the Vienna Wireless Testbed.

The signal is transmitted at a carrier frequency of $f_c = 2.4955\,\mathrm{GHz}$ with $L = 12$ subcarriers and a subcarrier spacing of $F = 15\,\mathrm{kHz}$, leading to a transmission bandwidth of $FL = 180\,\mathrm{kHz}$. The sampling rate is $f_s = 200\,\mathrm{MHz}$ (determined by the hardware) so that the FFT size becomes $\lceil \frac{f_s}{F} \rceil = 13334$, whereas most FFT points are set to zero. Similar as in Section IV and V, we consider three transmit blocks but evaluate the performance only for block 2. For FBMC, one block consists of $K = 32$ FBMC-symbols and a zero time-slot, leading to a transmission time of $(K+1)T = 1.1\,\mathrm{ms}$ per block. We also apply spreading in the time domain, as explained in Section III, so that we have 16 available symbols per subcarrier. For OFDM, the CP length is set to $T_{\mathrm{CP}} = 2.085\,\mu\mathrm{s}$, approximately half the length of that in LTE, and the number of time-symbols per block is set to $K = 16$, leading to the same transmission time as in FBMC, that is, $K(1/F + T_{\mathrm{CP}}) = 1.1\mathrm{ms}$. We therefore have the same bit rate for FBMC and OFDM, allowing a fair comparison, although we should keep in mind that FBMC has better spectral properties so that a higher number of subcarriers could be used. Note that the SNR in FBMC is 0.13 dB better than in OFDM because the zero time-slots require no power. In real world transmissions, channel estimation is always necessary, which we perform by pilot symbol aided channel estimation, similar as in LTE, that is, a diamond shaped pilot pattern with eight pilot symbols per antenna. Because the channel is highly correlated in time and frequency, we average over all eight channel estimates, improving the channel estimation accuracy. At the pilot positions of antenna 1, antenna 2 must transmit zero symbols in order to avoid interference. The same applies in reversed order. Thus, we lose 16 data symbols for the channel estimation, so that, for 16-QAM, 704 bits are transmitted per antenna (spatial multiplexing). The receiver is located indoor while the transmitter is 150 m away, on the rooftop of the opposite building [10]. We obtain different MIMO channel realizations by relocating the static receive antennas to 1024 positions within a 4×4 wavelength grid.

For 2×2 spatial multiplexing, we transmit independent bit streams at both antennas simultaneously. At the receiver, we detect the transmitted symbols either by zero-forcing equalization, which has the disadvantage of noise enhancement, or by Maximum Likelihood (ML) detection [5], which requires a higher computational complexity. Our ML detection assumes perfect channel knowledge and Gaussian distributed noise, so that we only approximate the true ML performance. Note

$$\mathbf{D} = \begin{bmatrix} 1 & +\mathrm{j}0.4357 & +\mathrm{j}0.4357 & +\mathrm{j}0.2393 & 0 & +\mathrm{j}0.0369 & +\mathrm{j}0.0098 & +\mathrm{j}0.0054 \\ -\mathrm{j}0.4357 & 1 & -\mathrm{j}0.2393 & -\mathrm{j}0.4357 & -\mathrm{j}0.0369 & 0 & -\mathrm{j}0.0054 & -\mathrm{j}0.0098 \\ -\mathrm{j}0.4357 & +\mathrm{j}0.2393 & 1 & +\mathrm{j}0.4357 & +\mathrm{j}0.4357 & +\mathrm{j}0.2393 & 0 & +\mathrm{j}0.0369 \\ -\mathrm{j}0.2393 & +\mathrm{j}0.4357 & -\mathrm{j}0.4357 & 1 & -\mathrm{j}0.2393 & -\mathrm{j}0.4357 & -\mathrm{j}0.0369 & 0 \\ 0 & +\mathrm{j}0.0369 & -\mathrm{j}0.4357 & +\mathrm{j}0.2393 & 1 & +\mathrm{j}0.4357 & +\mathrm{j}0.4357 & +\mathrm{j}0.2393 \\ -\mathrm{j}0.0369 & 0 & -\mathrm{j}0.2393 & +\mathrm{j}0.4357 & -\mathrm{j}0.4357 & 1 & -\mathrm{j}0.2393 & -\mathrm{j}0.4357 \\ -\mathrm{j}0.0098 & +\mathrm{j}0.0054 & 0 & +\mathrm{j}0.0369 & -\mathrm{j}0.4357 & +\mathrm{j}0.2393 & 1 & +\mathrm{j}0.4357 \\ -\mathrm{j}0.0054 & +\mathrm{j}0.0098 & -\mathrm{j}0.0369 & 0 & -\mathrm{j}0.2393 & +\mathrm{j}0.4357 & -\mathrm{j}0.4357 & 1 \end{bmatrix} \quad (22)$$

that ML detection is not feasible in conventional FBMC because too many possibilities have to be calculated due to the imaginary interference. The second transmission scheme we consider is 2×1 Alamouti's space-time block code [9] which achieves full diversity at rate one. Figure 8 shows the measured bit error ratio over the SNR (see [11] for our SNR definition). FBMC and OFDM have the same performance which validates that our FBMC spreading approach works in real world scenarios.

VII. Conclusion

MIMO works perfectly well in FBMC-OQAM once we spread symbols in the time (or frequency) domain, with approximately the same MIMO complexity as in OFDM. Because wireless channels are highly underspread, such FBMC based MIMO transmission works in many real world scenarios, as validated by our testbed measurements. If block wise transmission is required, we suggest the usage of guard slots in order to increase the SIR.

Appendix

For a better understanding of our notations and the underlying concept, we provide a simple example for the special case of $L = 2$ subcarriers and $K = 4$ FBMC symbols. The transmission matrix in (8) can then be expressed by (22). Note that $[\mathbf{D}]_{1,2}$ and $[\mathbf{D}]_{1,3}$ have both the same values. This means, that the interference from neighboring subcarriers has the same influence as the interference from neighboring FBMC symbols. This is caused by our prototype filter which has the same shape in time and in frequency due to the Hermite polynomials, see [13].

Using the Hadamard spreading approach, described in Section III, we find the coding matrix according to:

$$\mathbf{C} = \frac{1}{2} \begin{bmatrix} 1 & 0 & 1 & 0 \\ 0 & 1 & 0 & 1 \\ 1 & 0 & -1 & 0 \\ 0 & -1 & 0 & 1 \\ 1 & 0 & -1 & 0 \\ 0 & 1 & 0 & -1 \\ 1 & 0 & 1 & 0 \\ 0 & -1 & 0 & -1 \end{bmatrix}. \quad (23)$$

Note that many elements in $\mathbf{C}$ are zero, which reflects the fact that we spread over time only, see (5) and (6) for the underlying structure. It can easily be validated that the condition in (12) holds, that is, $\mathbf{C}^{\mathsf{H}}\,\mathbf{D}\,\mathbf{C} = \mathbf{I}$.

Acknowledgment

The financial support by the Austrian Federal Ministry of Science, Research and Economy, the National Foundation for Research, Technology and Development, and the TU Wien is gratefully acknowledged.

References

[1] G. Wunder, P. Jung, M. Kasparick, T. Wild, F. Schaich, Y. Chen, S. Brink, I. Gaspar, N. Michailow, A. Festag *et al.*, "5GNOW: non-orthogonal, asynchronous waveforms for future mobile applications," *IEEE Communications Magazine*, vol. 52, no. 2, pp. 97–105, 2014.

[2] F. Schaich, T. Wild, and Y. Chen, "Waveform contenders for 5G-suitability for short packet and low latency transmissions," in *IEEE Vehicular Technology Conference (VTC Spring)*, 2014, pp. 1–5.

[3] B. Farhang-Boroujeny, "OFDM versus filter bank multicarrier," *IEEE Signal Processing Magazine*, vol. 28, no. 3, pp. 92–112, 2011.

[4] R. Nissel and M. Rupp, "Bit error probability for pilot-symbol aided channel estimation in FBMC-OQAM," in *IEEE International Conference on Communications (ICC)*, Kuala Lumpur, Malaysia, May 2016.

[5] R. Zakaria and D. Le Ruyet, "A novel filter-bank multicarrier scheme to mitigate the intrinsic interference: application to MIMO systems," *IEEE Trans. Wireless Commun.*, vol. 11, no. 3, pp. 1112–1123, 2012.

[6] M. Payaró, A. Pascual-Iserte, and M. Nájar, "Performance comparison between FBMC and OFDM in MIMO systems under channel uncertainty," in *IEEE European Wireless Conference (EW)*, 2010.

[7] P. Chevalier, D. L. Ruyet, and R. Chauvat, "Maximum likelihood alamouti receiver for filter bank based multicarrier transmissions," *International ITG Workshop on Smart Antennas (WSA)*, 2016.

[8] C. Lélé, P. Siohan, R. Legouable, and M. Bellanger, "CDMA transmission with complex OFDM/OQAM," *EURASIP Journal on Wireless Communications and Networking*, vol. 2008, p. 18, 2008.

[9] C. Lélé, P. Siohan, and R. Legouable, "The alamouti scheme with CDMA-OFDM/OQAM," *EURASIP Journal on Advances in Signal Processing*, vol. 2010, no. 1, p. 1, 2010.

[10] R. Nissel, M. Lerch, and M. Rupp, "Experimental validation of the OFDM bit error probability for a moving receive antenna," in *IEEE Vehicular Technology Conference (VTC)*, Vancouver, Canada, Sept 2014.

[11] R. Nissel, S. Caban, and M. Rupp, "Experimental evaluation of FBMC-OQAM channel estimation based on multiple auxiliary symbols," in *IEEE Sensor Array and Multichannel Signal Processing Workshop (SAM)*, Rio de Janeiro, Brazil, July 2016.

[12] H. G. Feichtinger and T. Strohmer, *Gabor analysis and algorithms: Theory and applications*. Springer Science & Business Media, 2012.

[13] R. Nissel and M. Rupp, "On pilot-symbol aided channel estimation in FBMC-OQAM," in *IEEE International Conference on Acoustics, Speech and Signal Processing (ICASSP)*, Shanghai, China, March 2016.

[14] M. Bellanger, D. Le Ruyet, D. Roviras, M. Terré, J. Nossek, L. Baltar, Q. Bai, D. Waldhauser, M. Renfors, T. Ihalainen *et al.*, "FBMC physical layer: a primer," *PHYDYAS, January*, 2010.

[15] H. Nam, M. Choi, C. Kim, D. Hong, and S. Choi, "A new filter-bank multicarrier system for QAM signal transmission and reception," in *IEEE International Conference on Communications (ICC)*, 2014.

[16] Y. H. Yun, C. Kim, K. Kim, Z. Ho, B. Lee, and J.-Y. Seol, "A new waveform enabling enhanced QAM-FBMC systems," in *IEEE International Workshop on Signal Processing Advances in Wireless Communications (SPAWC)*, 2015, pp. 116–120.

[17] G. Matz, H. Bolcskei, and F. Hlawatsch, "Time-frequency foundations of communications: Concepts and tools," *IEEE Signal Processing Magazine*, vol. 30, no. 6, pp. 87–96, 2013.